

# Zinc and cadmium complexes with versatile hexadentate Schiff base ligands. The supramolecular self-assembly of a 3-D cage-like complex †

Jesús Sanmartín, Manuel R. Bermejo,\* Ana M. García-Deibe, Ivana M. Rivas and Ana R. Fernández

*Dpto. de Química Inorgánica, Facultad de Química, Campus Sur, Universidade de Santiago de Compostela, E-15706 Santiago de Compostela, Galicia, Spain.  
E-mail: qisuso@usc.es*

Received 6th July 2000, Accepted 20th September 2000  
First published as an Advance Article on the web 30th October 2000

Mono- and poly-nuclear neutral complexes have been obtained by electrochemical reaction of zinc or cadmium anodes with potentially hexadentate ligands  $H_4L^n$  ( $n=1-3$ ). The ligands were prepared by 2:1 condensation of 3-hydroxysalicylaldehyde and 1,2-diaminopropane, 1,3-diaminopropane or 1,4-diaminobutane, respectively. They can act either as  $N_2O_2$  dianionic in mononuclear complexes or as  $N_2O_4$  tetraanionic in polynuclear complexes, where metal ions are held together by  $\mu$ -phenoxo bridges. X-Ray diffraction study of self-assembled  $[Zn_8(L^3)_4(H_2O)_3] \cdot H_2O \cdot \frac{1}{4}MeCN$  shows a 3-D cage-like crystal structure, where the ligand units display  $O_2 + N_2O_2 + O_2$  polynucleating behaviours.

## Introduction

Synthesis of polynuclear metal complexes based on the development of multicomponent supramolecular structures is a rapidly growing area of research.<sup>1</sup> The use of compartmental ligands, capable of holding metal ions in close proximity, is of importance for this purpose.<sup>2</sup>

A large number of polynuclear S-bridged zinc complexes are described in the literature,<sup>3</sup> but O-bridged ones are much more scarce. Bis(3-hydroxy or 3-methoxy) derivatives of salen or salpn [ $H_2salpn = N,N$ -bis(salicylidene)propane-1,2-diamine]<sup>4-6</sup> can bind d- and f-metal ions to their inner  $N_2O_2$  and outer  $O_4$  sites, respectively. It was also reported that some of these hexadentate Schiff bases can simultaneously co-ordinate d ions in both compartments.<sup>7</sup> In this way, ligands derived from 3-hydroxysalicylaldehyde and several simple diamines such as 1,2-diaminoethane, 1,2-diamino-2-methylpropane or 1,3-diamino-2,2-dimethylpropane, have been used to prepare some  $N_2O_2$  mononuclear and  $N_2O_2 + O_4$  binuclear complexes. The latter mostly contain  $Cu^{II}$ ,  $Ni^{II}$  or  $Fe^{III}$  in the inner chamber and  $Mn^{II}$ ,  $Co^{II}$  or  $Fe^{III}$  in the outer compartment.<sup>7</sup> A few binuclear complexes of  $Cu^{II}$  and  $Zn^{II}$  are described with zinc ion co-ordinated in the outer  $O_4$  compartment.

Our approach to polynuclear complexes has been based on this type of compartmental Schiff base and making use of an electrochemical synthetic method. Recently, we have been able to synthesize, mono- and homopoly-nuclear complexes of Zn and Cd with a polyhydroxyl salpn derivative.<sup>8</sup> Now, we report the co-ordinating behaviour, towards Zn and Cd, of some related ligands with three different spacer lengths, so that their flexibility and/or size of compartment could influence their arrangement. The  $H_4L^3$  ligand has been demonstrated to be very versatile, since it can act either as dianionic, behaving as  $ON + NO$  binucleating,<sup>9</sup> or as tetraanionic, behaving as  $O_2 + N_2O_2 + O_2$  tri-, tetra- or even penta-nucleating.<sup>10</sup> Its four-membered methylene chain can provide a substantial flexibility, and this fact seems to contribute to the appearance

of high nuclearity.<sup>9-12</sup> The crystal structure found for  $[Zn_8(L^3)_4(H_2O)_3] \cdot H_2O \cdot \frac{1}{4}MeCN$ ,<sup>10</sup> which forms a small 3-D cage, is rather unusual too, and one of the rare and recent examples of oxo-bridged octanuclear zinc(II) complexes.<sup>11,13</sup>

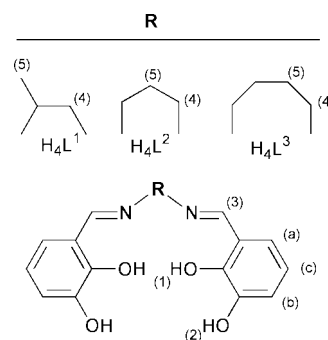


Chart 1

## Results and discussion

### Complexes synthesis and their solution stability

The anodic oxidation of zinc and cadmium in the presence of  $H_4L^n$  ( $n=1-3$ ) is a direct and efficient route to homopoly-nuclear compounds of the type  $[M_2(L^n)(H_2O)_x]_n$  ( $x=1-3$ ). The reduction of the duration of the electrochemical process to half allows one to obtain the corresponding mononuclear complexes,  $M(H_2L^n)(H_2O)_x$  ( $x=2$  or  $3$ ). The high yields and experimental data are collected in Table 1. In keeping with our previous practice,<sup>8,14</sup> we have measured the electrochemical efficiency  $E_f$ , which is defined as the quantity of metal dissolved per farad of charge. The  $E_f$  values are close to  $0.5 \text{ mol F}^{-1}$  and in accordance with a one-step mechanism for the redox reaction at the anode.

Analytical data, deposited as ESI, allow us to postulate empirical formulae of the types  $M_2(L^n)(H_2O)_x$  and  $M(H_2L^n)(H_2O)_x$  for the complexes. The complexes have been studied by thermal analysis, infrared, mass and <sup>1</sup>H NMR spectrometries and X-ray diffraction techniques, in appropriate cases.

† Electronic supplementary information (ESI) available: elemental analysis data. See <http://www.rsc.org/suppdata/dt/b0/b005421f/>

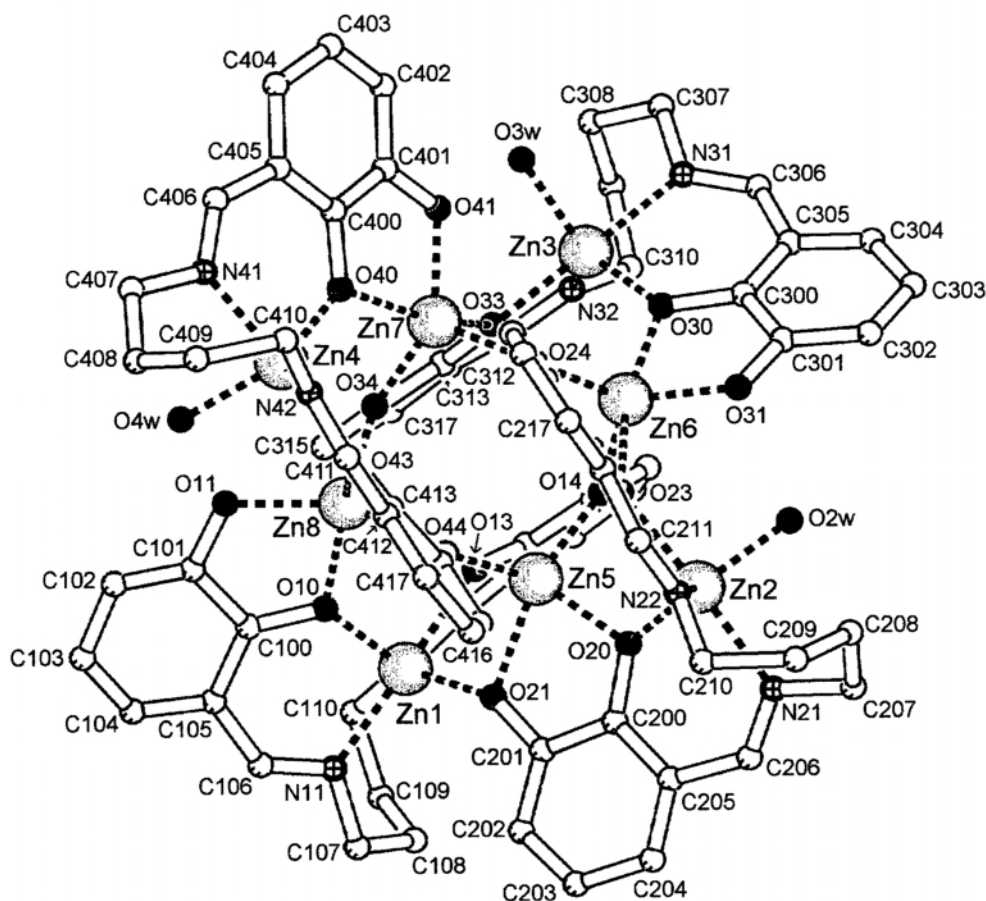


**Fig. 1** Molecular structure of  $[\text{Zn}_8(\text{L}^3)_4(\text{H}_2\text{O})_3] \cdot \text{H}_2\text{O} \cdot \frac{1}{4}\text{MeCN}$  showing the cage cavity and the stacked aromatic rings. Some labels are omitted for clarity, but the numbering scheme is systematic, as Fig. 4(c) and 4(d) show.

**Table 1** Experimental conditions used in the synthesis of the complexes

Complex	Amount $\text{H}_4\text{L}^n/\text{g}$	Electrolysis time <sup>a</sup> /h min	Initial voltage <sup>b</sup> /V	Yield (%)
$\text{Zn}(\text{H}_2\text{L}^1)(\text{H}_2\text{O})_2$	0.200	3:24	12.0	74
$[\text{Zn}_2(\text{L}^1)(\text{H}_2\text{O})]_n$	0.088	3:00	7.5	82
$\text{Cd}(\text{H}_2\text{L}^1)(\text{H}_2\text{O})_2$	0.100	1:42	10.0	74
$[\text{Cd}_2(\text{L}^1)(\text{H}_2\text{O})_3]_n$	0.100	3:24	10.1	73
$\text{Zn}(\text{H}_2\text{L}^2)(\text{H}_2\text{O})_3$	0.200	3:24	8.0	87
$[\text{Zn}_2(\text{L}^2)(\text{H}_2\text{O})]_n$	0.089	3:00	9.5	85
$\text{Cd}(\text{H}_2\text{L}^2)(\text{H}_2\text{O})_2$	0.100	1:42	10.0	76
$[\text{Cd}_2(\text{L}^2)(\text{H}_2\text{O})_2]_n$	0.100	3:24	9.8	70
$\text{Zn}(\text{H}_2\text{L}^3)(\text{H}_2\text{O})_2$	0.100	1:42	8.0	81
$[\text{Zn}_2(\text{L}^3)(\text{H}_2\text{O})]_n$	0.092	3:00	10.0	84
$\text{Cd}(\text{H}_2\text{L}^3)(\text{H}_2\text{O})_2$	0.100	1:42	9.6	82
$[\text{Cd}_2(\text{L}^3)(\text{H}_2\text{O})_2]_n$	0.100	3:24	9.6	87

<sup>a</sup> Calculated in accordance with the appropriate amount of ligand, for the processes  $2\text{M}(\text{s}) + \text{H}_4\text{L}^n(\text{MeCN}) \longrightarrow [\text{M}_2(\text{L}^n)(\text{H}_2\text{O})_x]_n + 2\text{H}_2(\text{g})$  and  $\text{M}(\text{s}) + \text{H}_4\text{L}^n(\text{MeCN}) \longrightarrow \text{M}(\text{H}_2\text{L}^n)(\text{H}_2\text{O})_x + \text{H}_2(\text{g})$ . <sup>b</sup> To produce a current of 10 mA.

The powdery compounds isolated are light and air stable but, in aqueous solution, polynuclear complexes yield mixtures of hydrolysed compounds. Thus, microanalyses of several mixtures, which were consecutively isolated from water or ethanol solutions of  $[\text{Zn}_2(\text{L}^3)(\text{H}_2\text{O})]_n$ , showed a gradual decrease of the C, H, and N percentage values. Likewise, their corresponding IR spectra show an increase of  $\nu(\text{O}-\text{H})$  intensity, as well as the appearance of a new band near  $1060\text{ cm}^{-1}$ , attributable to the ZnOH bending mode.<sup>15</sup>

The solution stability of the mononuclear complexes could also be illustrated by electrolysis of  $\text{Zn}(\text{H}_2\text{L}^3)(\text{H}_2\text{O})_2$  (in dmsO solution during 1 h 10 min, at 8 V and 5 mA) in the presence

of a cadmium anode. This resulted in a new compound with empirical formula  $[\text{Cd}_2(\text{L}^3)(\text{H}_2\text{O})]_n$ . The process seems to involve a transmetalation reaction<sup>16</sup> via an electrochemical technique, as we have previously reported.<sup>8</sup>

#### Crystal structure of $[\text{Zn}_8(\text{L}^3)_4(\text{H}_2\text{O})_3] \cdot \text{H}_2\text{O} \cdot \frac{1}{4}\text{MeCN}$

A preliminary account of  $[\text{Zn}_8(\text{L}^3)_4(\text{H}_2\text{O})_3] \cdot \text{H}_2\text{O} \cdot \frac{1}{4}\text{MeCN}$  has recently been published.<sup>10</sup> However, a more detailed discussion can be useful to illustrate the versatile and peculiar co-ordinating behaviour of  $\text{H}_4\text{L}^3$  in polynuclear complexes.<sup>9,10</sup> Selected distances and angles are listed in Tables 2 and 3, respectively.

The X-ray diffraction studies have revealed that, in this octanuclear neutral complex, Zn atoms are five-co-ordinated and form a singular 3-D cage-like complex (Fig. 1). The apical zinc atoms [Zn(1)–Zn(4)] of the pseudo-tetrahedral core (Fig. 2) are in slightly distorted trigonal-bipyramidal  $\text{N}_2\text{O}_3$  chromophores, where the  $\text{N}_2\text{O}_2$  inner compartment of each  $(\text{L}^3)^{4-}$  unit and a co-ordinated water molecule, or a  $\mu$ -phenoxo bridge, complete the co-ordination polyhedrons. An azomethine N atom [N(11), N(21), N(31) and N(41)] and an inner phenolic O atom of each  $(\text{L}^3)^{4-}$  unit [O(13), O(23), O(33) and O(43)] occupy their axial positions.

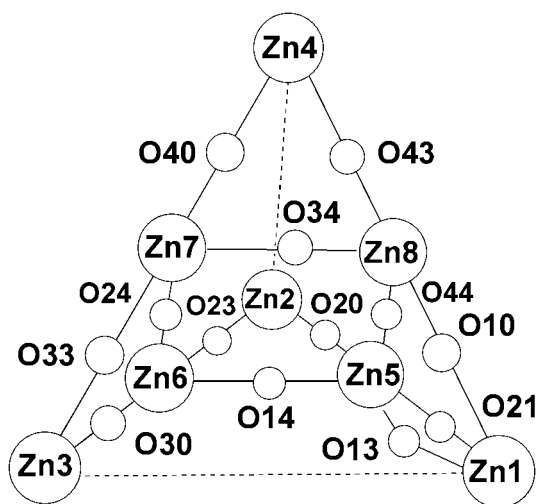
The other four metal centres Zn(*x*), *x* = 5–8, are in  $\text{O}_3$  chromophores, which are formed only by phenolic O atoms corresponding to three different ligand units. The  $\tau$  values<sup>17</sup> found for Zn(5), Zn(7) and Zn(8) ( $\tau$  0.018, 0.327 and 0.032, respectively) are indicative of a square pyramidal geometry, where the metal ion is displaced [0.723(3), 0.594(3) and 0.615(3) Å, respectively] from the square-base plane towards the pyramid centre. Both phenolic O atoms of the same aldehyde residue, corresponding to two different ligand units, form the opposite edges of each square base of the pyramid. The axial

**Table 2** Selected interatomic distances (Å) for  $[\text{Zn}_8(\text{L}^3)_4(\text{H}_2\text{O})_3] \cdot \text{H}_2\text{O} \cdot \frac{1}{4}\text{MeCN}$  with e.s.d.s in parentheses

Zn(1)–O(10)	1.966(6)	Zn(5)–O(44)	1.928(6)	Zn(1)⋯Zn(5)	3.1816(17)
Zn(1)–O(13)	2.036(6)	Zn(5)–O(20)	2.000(5)	Zn(1)⋯Zn(8)	3.6993(16)
Zn(1)–O(21)	2.054(6)	Zn(5)–O(14)	2.054(5)	Zn(2)⋯Zn(5)	3.3450(17)
Zn(1)–N(11)	2.064(10)	Zn(5)–O(13)	2.070(5)	Zn(2)⋯Zn(6)	3.8871(16)
Zn(1)–N(12)	2.144(10)	Zn(5)–O(21)	2.149(6)	Zn(3)⋯Zn(6)	3.5654(16)
				Zn(3)⋯Zn(7)	3.9006(16)
Zn(2)–O(2w)	1.968(7)	Zn(6)–O(14)	1.945(5)	Zn(4)⋯Zn(8)	3.7373(15)
Zn(2)–O(20)	1.987(6)	Zn(6)–O(24)	1.974(5)	Zn(4)⋯Zn(7)	3.7805(16)
Zn(2)–N(22)	2.047(7)	Zn(6)–O(31)	1.974(6)	Zn(5)⋯Zn(6)	3.3754(16)
Zn(2)–O(23)	2.052(5)	Zn(6)–O(30)	2.081(5)	Zn(5)⋯Zn(8)	3.4089(17)
Zn(2)–N(21)	2.115(8)	Zn(6)–O(23)	2.328(5)	Zn(6)⋯Zn(7)	3.4242(17)
				Zn(7)⋯Zn(8)	3.4042(15)
Zn(3)–O(30)	1.990(6)	Zn(7)–O(41)	1.913(6)	N(11)⋯N(12)	3.018(16)
Zn(3)–O(3w)	1.997(6)	Zn(7)–O(34)	1.955(5)	O(10)⋯O(13)	2.765(9)
Zn(3)–N(32)	2.021(7)	Zn(7)–O(24)	1.959(5)	O(11)⋯O(14)	6.346(9)
Zn(3)–O(33)	2.089(5)	Zn(7)–O(40)	2.227(5)	O(21)⋯O(24)	5.918(8)
Zn(3)–N(31)	2.156(9)	Zn(7)–O(33)	2.296(5)		
				Significant hydrogen bonds	
Zn(4)–O(40)	2.007(5)	Zn(8)–O(34)	1.944(5)	O(2w)⋯O(31)	2.499
Zn(4)–N(42)	2.056(7)	Zn(8)–O(11)	1.982(7)	O(3w)⋯O(41)	2.545
Zn(4)–O(43)	2.059(5)	Zn(8)–O(44)	1.985(5)	O(4w)⋯O(11)	2.519
Zn(4)–O(4w)	2.071(6)	Zn(8)–O(10)	2.165(6)		
Zn(4)–N(41)	2.098(8)	Zn(8)–O(43)	2.171(5)		

**Table 3** Selected angles (°) for  $[\text{Zn}_8(\text{L}^3)_4(\text{H}_2\text{O})_3] \cdot \text{H}_2\text{O} \cdot \frac{1}{4}\text{MeCN}$  with e.s.d.s in parentheses

<i>TBPY</i> environments		Square pyramidal environments		Bridge angles	
O(13)–Zn(1)–N(11)	176.8(3)	O(44)–Zn(5)–O(13)	97.1(2)	Zn(1)–O(13)–Zn(5)	101.6(2)
O(10)–Zn(1)–O(21)	104.0(3)	O(44)–Zn(5)–O(14)	121.9(2)	Zn(1)–O(21)–Zn(5)	98.4(3)
O(10)–Zn(1)–N(12)	121.9(3)	O(44)–Zn(5)–O(20)	119.7(2)	Zn(1)–O(10)–Zn(8)	127.1(3)
O(21)–Zn(1)–N(12)	130.3(3)	O(44)–Zn(5)–O(21)	94.0(3)		
		O(20)–Zn(5)–O(13)	136.3(2)	Zn(2)–O(20)–Zn(5)	114.1(3)
O(23)–Zn(2)–N(21)	175.5(3)	O(21)–Zn(5)–O(14)	137.4(2)	Zn(2)–O(23)–Zn(6)	125.0(2)
O(20)–Zn(2)–N(22)	122.2(3)				
O(2w)–Zn(2)–N(22)	115.6(3)	O(24)–Zn(7)–O(33)	91.0(2)	Zn(3)–O(30)–Zn(6)	122.3(3)
O(2w)–Zn(2)–O(20)	122.2(3)	O(24)–Zn(7)–O(34)	110.9(2)	Zn(3)–O(33)–Zn(7)	125.5(2)
		O(24)–Zn(7)–O(40)	112.9(2)		
O(33)–Zn(3)–N(31)	178.2(3)	O(24)–Zn(7)–O(41)	110.4(3)	Zn(4)–O(40)–Zn(7)	126.4(2)
O(30)–Zn(3)–N(32)	121.3(3)	O(40)–Zn(7)–O(33)	155.6(2)	Zn(4)–O(43)–Zn(8)	124.1(3)
O(30)–Zn(3)–O(3w)	118.7(3)	O(41)–Zn(7)–O(34)	136.0(3)		
O(3w)–Zn(3)–N(32)	120.0(3)			Zn(5)–O(14)–Zn(6)	115.1(2)
		O(34)–Zn(8)–O(10)	118.0(2)	Zn(5)–O(44)–Zn(8)	121.2(3)
O(43)–Zn(4)–N(41)	176.0(3)	O(34)–Zn(8)–O(11)	104.1(3)		
O(40)–Zn(4)–N(42)	128.4(3)	O(34)–Zn(8)–O(43)	97.5(2)	Zn(6)–O(24)–Zn(7)	121.1(3)
O(40)–Zn(4)–O(4w)	116.3(3)	O(34)–Zn(8)–O(44)	109.1(2)	Zn(7)–O(34)–Zn(8)	121.6(5)
N(42)–Zn(4)–O(4w)	115.2(3)	O(10)–Zn(8)–O(43)	144.5(2)		
		O(11)–Zn(8)–O(44)	146.4(3)		
O(30)–Zn(6)–O(23)	162.3(2)				
O(14)–Zn(6)–O(31)	117.7(2)				
O(14)–Zn(6)–O(24)	114.2(2)				
O(24)–Zn(6)–O(31)	119.2(2)				

**Fig. 2** Schematic model for the pseudo-tetrahedral  $\text{Zn}_8\text{O}_{13}$  core.

position is occupied by the only O atom belonging to a third ligand unit [O(44), O(24) and O(34) for Zn(5), Zn(7) and Zn(8), respectively]. The Zn(6) environment can be considered as distorted *TBPY* [ $\tau = 0.718$  and O(30)–Zn(6)–O(23) 162.3(2)°]. Two inner phenolic oxygen atoms of two different ligand units are in their axial positions [O(30) and O(23)]. The outer phenolic oxygen atoms of the three different ligand units occupy the equatorial positions [O(31), O(24) and O(14)].

The Zn–N<sub>axial</sub> bonds [2.064(10)–2.156(7) Å] are similar to those described for other distorted *TBPY* zinc environments,<sup>11,18</sup> although Zn(3)–N(31) is slightly longer. The Zn–N<sub>equatorial</sub> lengths [2.021(7)–2.144(10) Å] are slightly shorter than the axial ones, but longer than those found for other polynuclear *TBPY* zinc(II) complexes containing a Schiff base.<sup>12</sup> The wide range of Zn–O lengths [1.913(6)–2.328(5) Å] is also found in other five-co-ordinated polynuclear zinc(II) complexes.<sup>11,12,18</sup>

With regard to the co-ordinating behaviours observed in polynuclear complexes,<sup>9,10</sup>  $\text{H}_4\text{L}^3$  seems to follow three trends: high  $\mu$ -O bridging ability; versatility, even showing two different

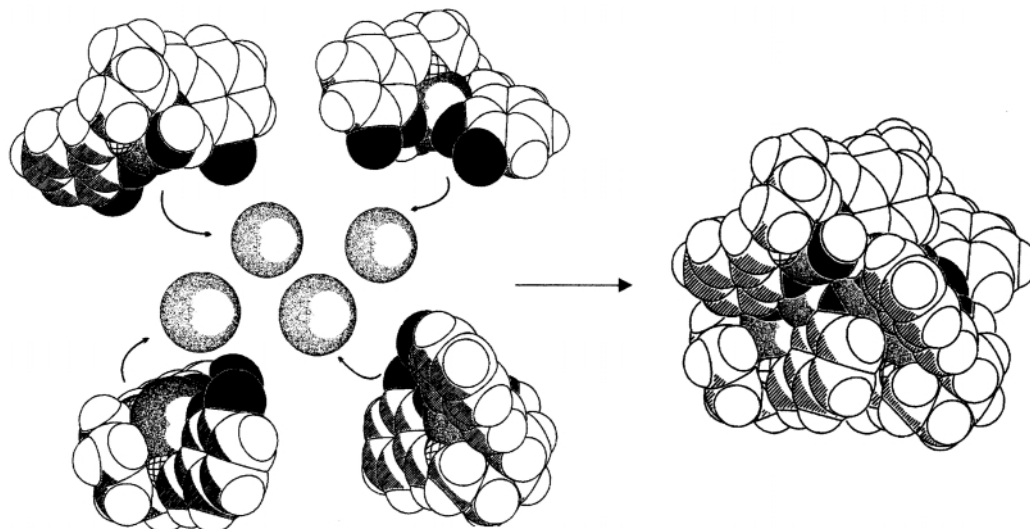


Fig. 3 Metal assisted self-assembly scheme based on a packing interaction, *via* phenolic atoms, of four mononuclear units with inner Zn( $x$ ),  $x = 5-8$ .

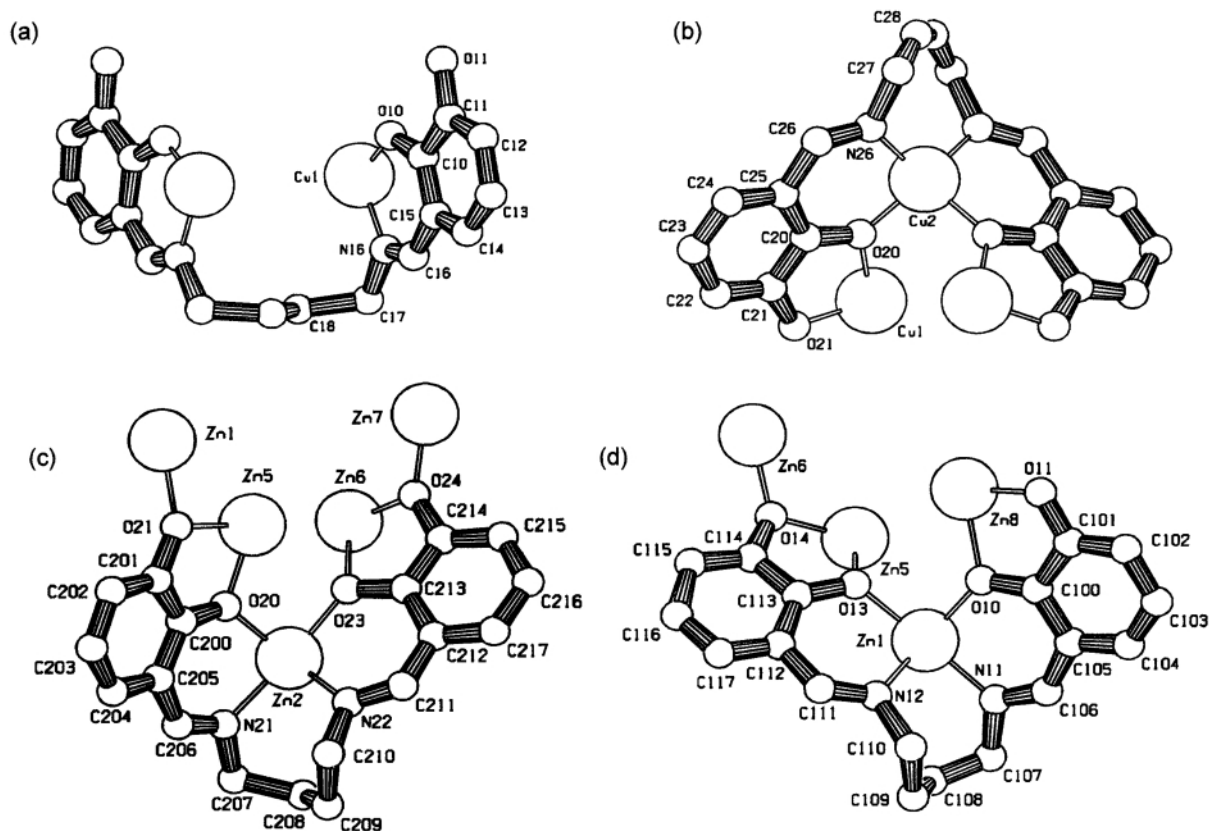


Fig. 4 (a)  $(\text{H}_2\text{L}^3)^{2-}$  acting as ON + NO binucleating in  $\text{Cu}_3(\text{H}_2\text{L}^3)(\text{L}^3)\cdot 2\text{H}_2\text{O}$ ; (b)  $(\text{L}^3)^{4-}$  acting as  $\text{O}_2 + \text{N}_2\text{O}_2 + \text{O}_2$  trinucleating in  $\text{Cu}_3(\text{H}_2\text{L}^3)(\text{L}^3)\cdot 2\text{H}_2\text{O}$ ; (c)  $(\text{L}^3)^{4-}$  acting as  $\text{O}_2 + \text{N}_2\text{O}_2 + \text{O}_2$  pentanucleating and (d) as tetranucleating in  $[\text{Zn}_8(\text{L}^3)_4(\text{H}_2\text{O})_3]\cdot \text{H}_2\text{O}\cdot \frac{1}{4}\text{MeCN}$ .

behaviours in the same complex, and flexibility, behaving as a helicand in some cases.

**High  $\mu$ -O bridging ligand ability.** An interesting feature of  $\text{H}_4\text{L}^3$  is the presence of four phenolic O atoms, which are responsible for the unusual high nuclearity observed in  $[\text{Zn}_8(\text{L}^3)_4(\text{H}_2\text{O})_3]\cdot \text{H}_2\text{O}\cdot \frac{1}{4}\text{MeCN}$ . This 3-D cage-like complex is assembled by means of thirteen  $\mu$ -phenoxo bridges, without the need of additional oxo or hydroxo bridging groups, as occurs in other cases.<sup>11-13,18,19</sup> The self-assembly is represented in Fig. 3. A central eight-membered square-like  $\text{Zn}_4\text{O}_4$  metallacycle, where Zn( $x$ ) ( $x = 5-8$ ) occupy its vertices, is observed in the pseudo-tetrahedral  $\text{Zn}_8\text{O}_{13}$  core. This  $\text{Zn}_4\text{O}_4$  metallacycle had previously been described for other O-bridged polynuclear cage<sup>11</sup> or macrocyclic<sup>12</sup> complexes.

The edges of the square-like metallacycle are shared with three six-membered  $\text{Zn}_3\text{O}_3$  metallacycles and a  $\text{Zn}_3\text{O}_4$  one. This last one is caused by the double  $\mu$ -phenoxo bridge between Zn(1) and Zn(5), leading to a significantly short Zn $\cdots$ Zn distance and subsequent distortion (Fig. 2). The rings are not planar, showing a slight "chair" conformation.

The central  $\text{Zn}_4\text{O}_4$  metallacycle surrounds the cage cavity, with Zn $\cdots$ Zn distances in the range 3.375(2)–3.424(2) Å. This small cavity could be accessible through the channel determined by the nearly parallel aromatic rings C(212)–C(217) and C(412)–C(417), and is almost perpendicular to the C(112)–C(117) and C(312)–C(317) rings. These are about 3.4–3.6 Å distant, which is indicative of a certain  $\pi$ – $\pi$  stacking (Fig. 1). These weak interactions, as well as hydrogen bonds, are usual in supramolecular assemblies, providing further stabilisation

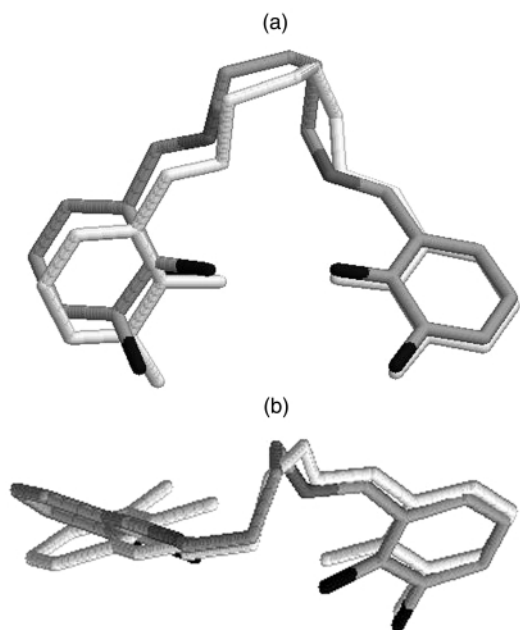


**Fig. 5** Perspective views of the (a) frontal and (b) lateral superimposition of two  $(L^3)^{4-}$  spatial arrangements: twisted in  $Cu_3(H_2L^3)(L^3) \cdot 2H_2O$  (pale) and slightly folded in  $[Zn_8(L^3)_4(H_2O)_3] \cdot H_2O \cdot \frac{1}{4}MeCN$  (dark).

to their arrangements. In our case, strong interactions between co-ordinated water molecules and neighbouring phenolic O atoms also seem to exist (Table 2).

**Ligand versatility.** The different co-ordination modes observed for the ligands used in this work is one of the subtle factors that can make unpredictable the metal assisted self-assembly.<sup>19–21</sup>

It is well known that  $N_2O_4$  Schiff bases with an ethylene or trimethylene spacer can show a  $N_2O_2$  mononucleating or a  $N_2O_2 + O_4$  binucleating behaviour.<sup>4,5</sup> We demonstrate here that a long tetramethylene spacer does not prevent the  $N_2O_2$  mononucleating behaviour of  $(H_2L^3)^{2-}$ , as is obvious from the  $^1H$  NMR spectrum of  $Zn(H_2L^3)(H_2O)_2$ .

Moreover, we had previously reported that in  $Cu_3(H_2L^3)(L^3) \cdot 2H_2O$ <sup>9</sup> the ligand units act in two rather different ways:  $(H_2L^3)^{2-}$  uses its inner compartment as ON + NO binucleating (Fig. 4a), whilst  $(L^3)^{4-}$  acts as  $O_2 + N_2O_2 + O_2$  trinucleating (Fig. 4b). Analogously, in  $[Zn_8(L^3)_4(H_2O)_3] \cdot H_2O \cdot \frac{1}{4}MeCN$ , the ligand units behave as  $O_2 + N_2O_2 + O_2$  polynucleating. Thus, the ligand unit which contains Zn(2) in its inner compartment is acting as pentanucleating (Fig. 4c), whereas the other three are behaving as tetranucleating (Fig. 4d).

Intramolecular distances between both azomethine N atoms and both inner phenolic O atoms found for  $(L^3)^{4-}$  in the octanuclear complex (Table 2), are similar to those observed for the trinuclear one [ $N \cdots N$  3.042(24) and  $O \cdots O$  2.830(17) Å]. However, outer phenolic O atoms for ligand units of the octanuclear complex are farther apart than in  $Cu_3(H_2L^3)(L^3) \cdot 2H_2O$  [5.787(18) Å].

**Ligand flexibility.** The flexible arrangement of  $H_4L^3$  in polynuclear complexes seems to be favoured by its long spacer. Two clearly different arrangements are displayed by the ligand in the [4 + 4 + 4] bischelate trinuclear copper(II) complex:<sup>9</sup>  $(H_2L^3)^{2-}$  is “step-like” (Fig. 4a) and  $(L^3)^{4-}$  a wrapping “loop” (Fig. 4b). The aliphatic chains of  $(L^3)^{4-}$  in  $[Zn_8(L^3)_4(H_2O)_3] \cdot H_2O \cdot \frac{1}{4}MeCN$  are even more twisted than in  $Cu_3(H_2L^3)(L^3) \cdot 2H_2O$ . This subtle difference, which is illustrated in Fig. 5, prevents their behaviour as typical helicands and seems to be an effect of the metal co-ordination geometry on the self-assembly.<sup>20,22,23</sup>

It was reported<sup>21</sup> that a change from a mononucleating to a polynucleating mode results in different geometries at metal centres and radically alters the assembly pathway to give polymeric rather than monomeric complexes. Here, a change from a trinucleating behaviour to tetra- or penta-nucleating gives a tetrameric 3-D cage-like and not a dimeric helical complex.

The marked torsion of  $(L^3)^{4-}$  leads to a loss of planarity that prevents the  $N_2O_2 + O_4$  co-ordinating behaviour. The two ON chelate planes of  $(L^3)^{4-}$  form an angle of 58.5(4)°, for the ligand containing Zn(1) in the  $N_2O_2$  compartment, whilst the two  $O_2$  chelate planes form an angle of 60.2(4)°. Similar values are observed for the other three ligand units, with the lowest and the highest values corresponding to those ligands containing Zn(4) and Zn(2) in their inner compartment, respectively. All these values are higher than those found for  $(L^3)^{4-}$  in the trinuclear copper(II) complex.

#### IR spectra

The most characteristic IR bands have been assigned following the literature<sup>4,7–8</sup> (Table 4). A comparison of the spectra of the “free” ligands and complexes in the range 1650–1200  $cm^{-1}$  indicates that the ligands are co-ordinated *via* N and O atoms. The  $\nu(C-N)$ ,  $\nu(C=O)$  and  $\nu(C-O)$  modes are present as three very strong bands at about 1640, 1460 and 1250  $cm^{-1}$ , respectively.

The sharp band due to the phenol OH groups appears at about 3220  $cm^{-1}$  for the “free” ligands. This disappears for the complexes and a very broad band at about 3400  $cm^{-1}$ , which is associated with co-ordinated or solvated water molecules, is now present. The presence of a sharp band corresponding to the remaining hydroxyl groups would be expected for mononuclear complexes, but it is obscured by the presence of water.

**Table 4** Some significant IR bands (in  $cm^{-1}$ ) and mass peaks (in  $m/z$ ) for the compounds

Compound	$\nu(O-H)$	$\nu(C=N)$	$\nu(C=O)$	$\nu(C-O)$	$m/z$ (% intensity)
$H_4L^1$	3238s, br	1625s	1464s	1273s	
$Zn(H_2L^1)(H_2O)_2$	3409s, br	1639s	1460s	1266s	378.0 (45)
$[Zn_2(L^1)(H_2O)]_n$	3426s, br	1635s	1453s	1262s	521.4 (30)
$Cd(H_2L^1)(H_2O)_2$	3422s, br	1628s	1448s	1250s	425.2 (31)
$[Cd_2(L^1)(H_2O)]_n$	3423s, br	1628s	1448s	1254s	
$H_4L^2$	3204s, br	1631s	1460s	1282s	
$Zn(H_2L^2)(H_2O)_3$	3402s, br	1638s	1460s	1253s	430.9 (100)
$[Zn_2(L^2)(H_2O)]_n$	3407s, br	1627s	1460s	1262s	563.3 (42)
$Cd(H_2L^2)(H_2O)_2$	3422s, br	1640s	1457s	1245s	463.0 (25)
$[Cd_2(L^2)(H_2O)]_n$	3422s, br	1623s	1456s	1248s	701.5 (28)
$H_4L^3$	3222s, br	1630s	1456s	1231s	
$Zn(H_2L^3)(H_2O)_2$	3386s, br	1640s	1458s	1245s	391.0 (36)
$[Zn_2(L^3)(H_2O)]_n$	3387s, br	1627s	1457s	1262s	579.2 (9)
$Cd(H_2L^3)(H_2O)_2$	3423s, br	1641s	1457s	1244s	
$[Cd_2(L^3)(H_2O)]_n$	3406s, br	1640s	1457s	1245s	

IR spectra were recorded as KBr pellets; s = strong; br = broad. Mass spectra were registered in acetonitrile solution.

**Table 5**  $^1\text{H}$  NMR data ( $\delta$ ) for ligands and complexes using  $\text{dms}\text{-d}_6$  as solvent

Compound	$\text{H}_{(1)}$	$\text{H}_{(2)}$	$\text{H}_{(3)}$	$\text{H}_{(a)}, \text{H}_{(b)}, \text{H}_{(c)}$	$\text{H}_{(4)}$	$\text{H}_{(5)}$
$\text{H}_4\text{L}^1$	13.52 (2H, br)	8.97 (2H, br)	8.56 (1H, s) 8.52 (1H, s)	6.85 (2H, d), 6.82 (2H, d), 6.66 (2H, t)	3.83 (2H, m) 3.81 (1H, m)	1.33 (3H, s)
$\text{Zn}(\text{H}_2\text{L}^1)(\text{H}_2\text{O})_2$		7.85 (2H, br)	8.46 (2H, s)	6.73 (2H, d), 6.71 (2H, d), 6.33 (2H, t)	3.89 (3H, m)	1.22 (3H, s)
$\text{Cd}(\text{H}_2\text{L}^1)(\text{H}_2\text{O})_2$		7.76 (2H, br)	8.30 (1H, s) 8.27 (1H, s)	6.69 (2H, d), 6.66 (2H, d), 6.25 (2H, t)	3.81 (3H, m)	1.26 (3H, s)
$\text{H}_4\text{L}^2$	13.66 (2H, br)	8.94 (2H, br)	8.53 (2H, s)	6.86 (2H, d), 6.84 (2H, d), 6.65 (2H, t)	3.72 (4H, m)	1.98 (2H, m)
$\text{Zn}(\text{H}_2\text{L}^2)(\text{H}_2\text{O})_3$		7.97 (2H, s)	8.24 (2H, s)	6.66 (2H, d), 6.63 (2H, d), 6.38 (2H, t)	3.60 (4H, m)	1.87 (2H, m)
$\text{Cd}(\text{H}_2\text{L}^2)(\text{H}_2\text{O})_2$			8.17 (2H, s)	6.62 (2H, d), 6.60 (2H, d), 6.25 (2H, t)	3.58 (4H, m)	1.91 (2H, m)
$\text{H}_4\text{L}^3$	13.81 (2H, br)	8.85 (2H, br)	8.53 (2H, s)	6.86 (2H, d), 6.83 (2H, d), 6.62 (2H, t)	3.66 (4H, m)	1.73 (4H, m)
$\text{Zn}(\text{H}_2\text{L}^3)(\text{H}_2\text{O})_2$		7.69 (2H, s)	8.37 (2H, s)	6.83 (2H, d), 6.71 (2H, d), 6.34 (2H, t)	3.60 (4H, m)	1.87 (4H, m)

br = broad, s = singlet, d = doublet, t = triplet, m = multiplet.

Therefore, no significant differences between the spectra of the mono- and their corresponding poly-nuclear complexes can be mentioned.

### $^1\text{H}$ NMR spectra

$^1\text{H}$  NMR spectra for ligands and mononuclear complexes were recorded in  $\text{DMSO-d}_6$ . The low solubility of  $\text{Cd}(\text{H}_2\text{L}^3)(\text{H}_2\text{O})_2$  and the polynuclear compounds, even in  $\text{py-d}_5$ , prevents their study. Assignment of signals (Table 5, Chart 1) was according to our experience<sup>8,24</sup> and the literature.<sup>5</sup> The symmetry of the ligands makes their spectra very simple (Fig. 6a). The aromatic protons in *ortho* and *para* positions with respect to the azomethine group are observed at low field ( $\delta$  6.85 and 6.82, respectively, for  $\text{H}_4\text{L}^1$ ). The signal corresponding to the aromatic proton in the *meta* position is slightly shifted to a higher field. Phenolic protons are detectable as two broad signals at low field ( $\Delta\delta$  about 5 ppm). Both protons  $\text{H}_{(3)}$  and  $\text{H}_{(4)}$  in  $\text{H}_4\text{L}^1$  display two signals caused by the asymmetry introduced by the presence of the methyl group in the aliphatic chain.

The absence of the  $\text{H}_{(1)}$  signal and the significant shift ( $\Delta\delta$  about 1 ppm) of the sharp signal corresponding to  $\text{H}_{(2)}$  for the mononuclear complexes confirm complexation of zinc ion in the inner  $\text{N}_2\text{O}_2$  compartment of the ligands. In general, an upfield shift is observed for all the proton signals after co-ordination. The most relevant feature is the slight shift ( $\Delta\delta$  about 0.1 ppm) observed for the  $\text{H}_{(3)}$  and methylenic protons, when compared with those of equivalent nickel(II) complex<sup>5</sup> ( $\Delta\delta$  about 0.7 ppm). This fact leads to an inversion of the relative positions of  $\text{H}_{(2)}$  and  $\text{H}_{(3)}$  in these zinc and cadmium complexes. This can clearly be observed in Fig. 6(b). The addition of  $\text{D}_2\text{O}$  to  $\text{Zn}(\text{H}_2\text{L}^2)(\text{H}_2\text{O})_2$  leads to the disappearance of the  $\text{H}_{(2)}$  signal, corroborating the correct assignment of OH protons, as Fig. 6(c) shows.

This spectroscopic study demonstrates that the three ligands show similar behaviour, forming  $\text{N}_2\text{O}_2$  mononuclear complexes, despite the differences between the ionic metal radii and the spacer group length.

### ES Mass spectra

Positive-ion electrospray mass spectra for the mononuclear complexes show peaks in the range  $m/z$  378–463 attributed to  $[\text{M}^+]$  or  $[\text{M} - 2\text{H}_2\text{O}]^+$ , that have been listed in Table 4. This is indicative of ligand co-ordination. A representative mass spectrum of a mononuclear complex is shown in Fig. 7(a). The low solubility of cadmium complexes makes their study difficult.

Except for  $[\text{Zn}_8(\text{L}^3)_4(\text{H}_2\text{O})_3] \cdot \text{H}_2\text{O} \cdot \frac{1}{4}\text{MeCN}$ , no  $\text{M}_2(\text{L})(\text{H}_2\text{O})_x$  fragments were detected in the spectra of the polynuclear complexes. The observation of peaks in the range  $m/z$  521–702 related to  $\text{M}_3(\text{L})(\text{H}_2\text{O})_x$  fragments could be indicative of at least a trinucleating behaviour displayed by the ligands. These facts are illustrated in Fig. 7(b) and suggest an  $\text{O}_2 + \text{N}_2\text{O}_2 + \text{O}_4$

polymeric behaviour of the ligands rather than a  $\text{N}_2\text{O}_2 + \text{O}_4$  monomeric one.

### DSC studies

Thermal analyses of the cadmium complexes show that they decompose without melting between 380 and 480 °C. The compounds lose water molecules under an air flux in the range 75–80 °C. This is in agreement with the presence of co-ordinated or/and solvated water in these complexes.

### Conclusion

The anodic oxidation of zinc and cadmium in the presence of  $\text{H}_4\text{L}^n$  is a direct and efficient route to homopolynuclear complexes. Shortening of the reaction times to half leads to the corresponding mononuclear complexes.

The ligands used here behave as dianionic  $\text{N}_2\text{O}_2$  tetradentate in mononuclear complexes and as tetraanionic hexadentate in polynuclear ones. Single crystal X-ray diffraction characterisation revealed that  $(\text{L}^3)^{4-}$  is acting as tetra- and exceptionally as penta-nucleating, by using its  $\text{O}_2 + \text{N}_2\text{O}_2 + \text{O}_2$  atom donor sets. This study also shows that the two ON chelate planes of the ligand inner compartment form angles higher than 50° in  $[\text{Zn}_8(\text{L}^3)_4(\text{H}_2\text{O})_3] \cdot \text{H}_2\text{O} \cdot \frac{1}{4}\text{MeCN}$ .

The flexible spacer group of  $\text{H}_4\text{L}^3$  is a crucial factor for the formation of supramolecular structures. This allows high nuclearity and different polynuclear architectures in the solid state, driven by factors such as the metal co-ordination requirements. Thus, subtle changes in its spatial arrangement, from a trinucleating to a tetra- or penta-nucleating behaviour, give a tetrameric 3-D cage-like instead of a bis-helical complex.

### Experimental

#### Materials

Metal anodes were used as sheets 0.5 mm thick. 2,3-Dihydroxybenzaldehyde, 1,2-diaminopropane, 1,3-diaminopropane and 1,4-diaminobutane were commercial products (Aldrich) used without further purification, as were the solvents.

#### Synthetic procedures

**Ligands.** The three ligands were obtained by the same synthesis procedure. That of  $\text{H}_4\text{L}^3$  is used as an example. A chloroform solution of 2,3-dihydroxybenzaldehyde (1.0 g, 0.724 mmol) and 1,4-diaminobutane (0.319 g, 0.362 mmol) was refluxed with a Dean–Stark condenser for 3 h. The yellow solid formed was filtered off, washed with diethyl ether and dried in vacuum. A hexane–acetone (10:1) solution was required for isolation of  $\text{H}_4\text{L}^1$  from the oil obtained in the condensation reaction.

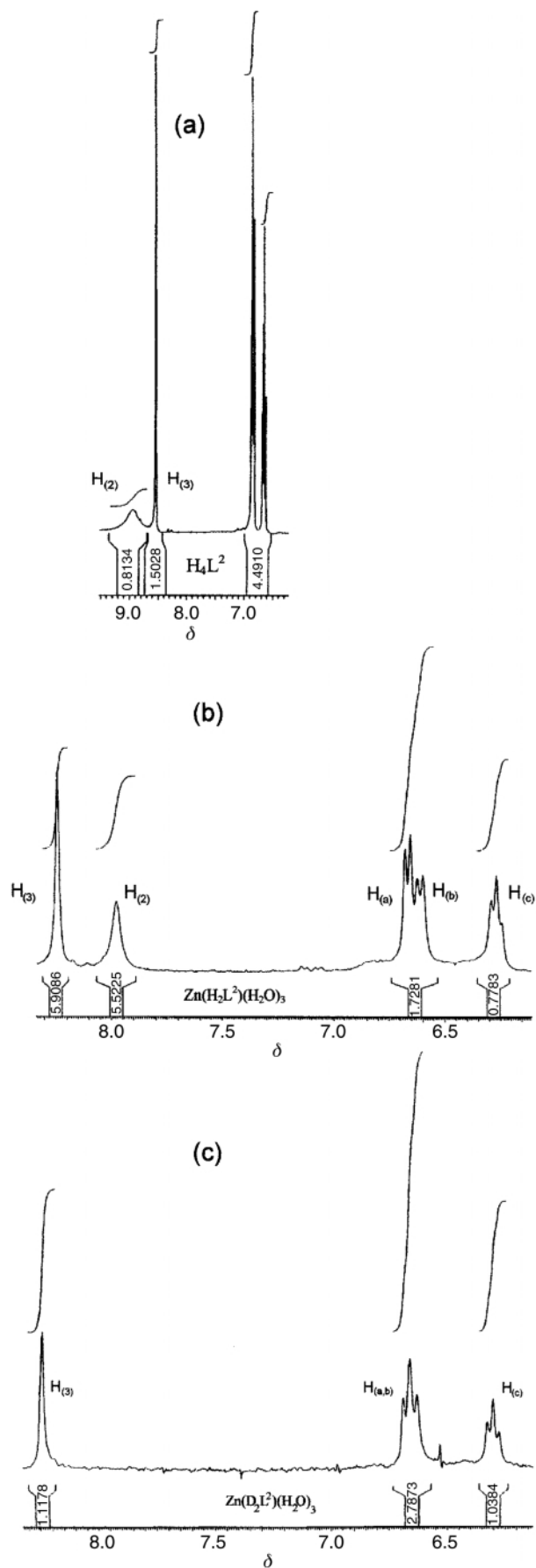


Fig. 6  $^1\text{H}$  NMR spectra (in the range  $\delta$  6.00–9.50) for: (a)  $\text{H}_4\text{L}^2$ , (b)  $\text{Zn}(\text{H}_2\text{L}^2)(\text{H}_2\text{O})_3$  and (c)  $\text{Zn}(\text{D}_2\text{L}^2)(\text{H}_2\text{O})_3$ .

**Complexes.** An electrochemical method was used in the synthesis of mono- and poly-nuclear complexes.<sup>8–10,25</sup> About 0.1 g of  $\text{H}_4\text{L}$  was dissolved with heating in *ca.* 80 mL of acetonitrile.

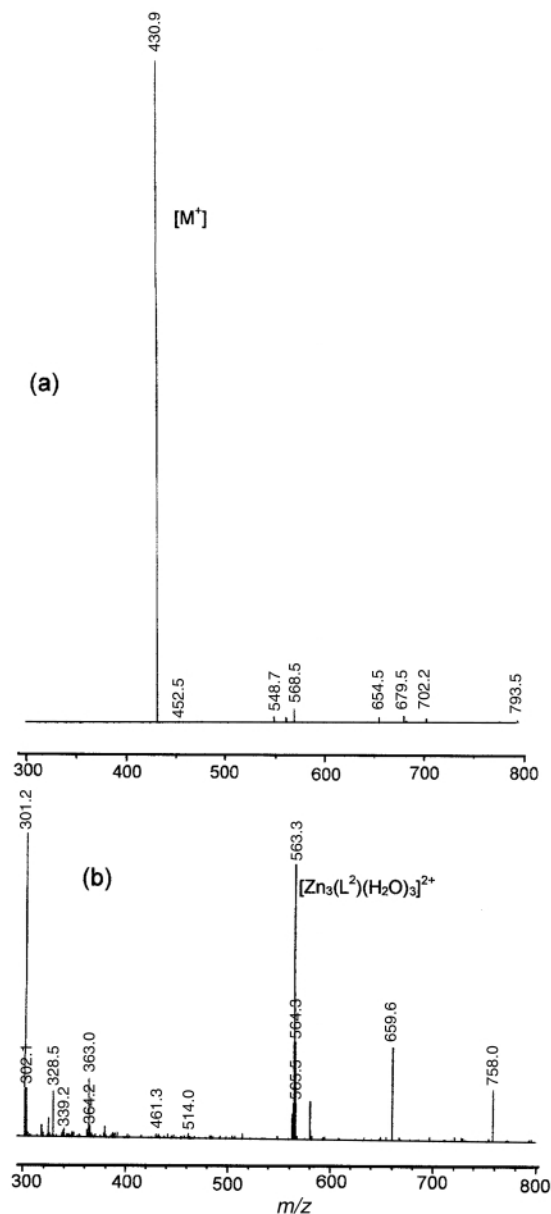


Fig. 7 Mass spectra (in the range  $m/z$  300–800) for (a)  $\text{Zn}(\text{H}_2\text{L}^2)(\text{H}_2\text{O})_3$  and (b)  $[\text{Zn}_2(\text{L}^2)(\text{H}_2\text{O})_n]$ .

Then, a small amount of tetramethylammonium perchlorate (*ca.* 30 mg) was added as supporting electrolyte. (**Caution:** Although no problem has been encountered in this work, all perchlorate compounds are potentially explosive, and should be handled in small quantities and with great care!) Applied voltages of 10–15 V (10 mA) allowed sufficient current flow for the solution of metals. The time of the electrolyses was calculated in accordance with the following reactions:  $\text{M}(\text{s}) + \text{H}_4\text{L} \rightarrow \text{M}(\text{H}_2\text{L})(\text{H}_2\text{O})_x + \text{H}_2(\text{g})$  and  $2\text{M}(\text{s}) + \text{H}_4\text{L} \rightarrow [\text{M}_2(\text{L})(\text{H}_2\text{O})_x]_n + 2\text{H}_2(\text{g})$ . In all cases hydrogen was evolved at the cathode. Cells can be summarised as:  $\text{M}_{(+)}|\text{MeCN} + \text{H}_4\text{L}|\text{Pt}_{(-)}$ . The experimental conditions are listed in Table 1. Solid products were easily isolated from the electrolysis solution by filtration. Insoluble products were washed with acetonitrile and diethyl ether to remove any excess of ligand. The solution obtained after filtration of  $[\text{Zn}_2(\text{L}^3)(\text{H}_2\text{O})_n]$  was evaporated at room temperature for a few days. Then small crystals of  $[\text{Zn}_8(\text{L}^3)_4(\text{H}_2\text{O})_3] \cdot \text{H}_2\text{O} \cdot \frac{1}{4}\text{MeCN}$  suitable for X-ray diffraction studies were collected.

#### Physicochemical measurements

Microanalyses were carried out by the in-house Elemental Analysis Service of the University of Santiago de Compostela

on a Fisons Instruments EA 1108 CHNS-O instrument. Infrared spectra were recorded, as KBr pellets, on a Mattson Galaxy FT-i.r.2020 spectrophotometer, NMR spectra in dms<sub>o</sub>-d<sub>6</sub> on a Bruker 300 AC spectrometer and ES mass spectra on a LC/MSD HP1100 spectrometer using acetonitrile as solvent. DSC thermograms were recorded in air by use of a PL differential scanning calorimeter and aluminium as reference. The temperature program was a ramp from 30 to 600 °C in 1 h.

## Acknowledgements

We would like to thank the Xunta de Galicia (Spain) (XUGA 20903B99).

## References

- 1 J. M. Lehn, *Supramolecular Chemistry*, VCH, Weinheim, 1995; E. C. Constable, in *Comprehensive Supramolecular Chemistry*, eds. J. P. Sauvage and M. W. Hosseini, Pergamon, Oxford, 1996, vol. 9, ch. 6.
- 2 P. A. Vigato, S. Tamburini and D. E. Fenton, *Coord. Chem. Rev.*, 1990, **106**, 25.
- 3 B. Krebs and G. Henkel, *Angew. Chem., Int. Ed. Engl.*, 1991, **30**, 769.
- 4 U. Casellato, P. Guerriero, S. Tamburini, S. Sitran and P. A. Vigato, *J. Chem. Soc., Dalton Trans.*, 1991, 2145.
- 5 U. Casellato, P. Guerriero, S. Tamburini, P. A. Vigato and C. Benelli, *Inorg. Chim. Acta*, 1993, **207**, 39.
- 6 J. P. Costes, F. Dahan, A. Dupuis and J. P. Laurent, *Inorg. Chem.*, 1996, **35**, 2400.
- 7 P. Guerriero, S. Tamburini, P. A. Vigato, U. Russo and C. Benelli, *Inorg. Chim. Acta*, 1993, **213**, 279.
- 8 J. Sanmartín, M. R. Bermejo, A. M. García-Deibe, M. Maneiro, C. Lage and A. J. Costa-Filho, *Polyhedron*, 2000, **19**, 185.
- 9 J. Sanmartín, M. R. Bermejo, A. M. García-Deibe, O. Piro and E. E. Castellano, *Chem. Commun.*, 1999, 1953.
- 10 J. Sanmartín, M. R. Bermejo, A. M. García-Deibe and A. Llamas, *Chem. Commun.*, 2000, 795.
- 11 M. Mikuriya, N. Tsuru, S. Ikemi and S. Ikenoue, *Chem. Lett.*, 1998, 879.
- 12 E. Asato, H. Furutachi, T. Kawahashi and M. Milkuriya, *J. Chem. Soc., Dalton Trans.*, 1995, 3897.
- 13 R. W. Saafrank, N. Low, S. Trummer, G. M. Sheldrick, M. Teichert and D. Stalke, *Eur. J. Inorg. Chem.*, 1998, 559.
- 14 J. Sanmartín, M. R. Bermejo, J. A. García-Vázquez, J. Romero, A. Sousa, A. Brodbeck, A. Castiñeiras, W. Hiller and J. Strähle, *Z. Naturforsch., Teil B*, 1993, **48**, 431.
- 15 M. Maltese and W. J. Orville-Thomas, *J. Inorg. Nucl. Chem.*, 1967, **29**, 2533.
- 16 S. Brooker, R. J. Kelly and P. G. Plieger, *Chem. Commun.*, 1998, 1079; H. Adams, N. A. Bailey, S. R. Collinson, D. E. Fenton, J. C. Kitchen and J. S. Kitchen, *J. Organomet. Chem.*, 1998, **550**, 7.
- 17 C. Bolos, P. C. Christidis, G. Will and L. Wiehl, *Inorg. Chim. Acta*, 1996, **248**, 209.
- 18 M. Mikuriya and S. Tashima, *Polyhedron*, 1998, **17**, 207.
- 19 F. A. Cotton, L. M. Daniels, L. R. Falvello, J. H. Matonic, C. A. Murillo, X. Wang and H. Zhou, *Inorg. Chim. Acta*, 1997, **266**, 91.
- 20 N. Yoshida, K. Ichikawa and M. Shiro, *J. Chem. Soc., Perkin Trans. 2*, 2000, 17.
- 21 R. L. Paul, A. J. Amoroso, P. L. Jones, S. M. Couchman, Z. R. Reeves, L. H. Rees, J. C. Jeffery, J. A. McCleverty and M. D. Ward, *J. Chem. Soc., Dalton Trans.*, 1999, 1563.
- 22 R. Ziessel, A. Harriman, J. Suffert, M. T. Youinou, A. De Cian and J. Fischer, *Angew. Chem., Int. Ed. Engl.*, 1997, **36**, 2509; M. J. Hannon, C. L. Painting, A. Jackson, J. Hamblin and W. Errington, *Chem. Commun.*, 1997, 1807; M. J. Hannon, S. Bunce, A. J. Clark and N. W. Alcock, *Angew. Chem., Int. Ed.*, 1999, **38**, 1277; M. J. Hannon, C. L. Painting and N. W. Alcock, *Chem. Commun.*, 1999, 2023.
- 23 N. Yoshida, H. Oshio and T. Ito, *J. Chem. Soc., Perkin Trans. 2*, 1999, 975; B. J. McNelis, L. C. Nathan and C. J. Clark, *J. Chem. Soc., Dalton Trans.*, 1999, 1831.
- 24 M. R. Bermejo, M. Fondo, A. García-Deibe, M. Rey, J. Sanmartín, A. Sousa, M. Watkinson, C. A. McAuliffe and R. G. Pritchard, *Polyhedron*, 1996, **15**, 4185.
- 25 M. R. Bermejo, M. Fondo, A. M. González, O. L. Hoyos, A. Sousa, C. A. McAuliffe, W. Hussein, R. G. Pritchard and V. M. Novotorsev, *J. Chem. Soc., Dalton Trans.*, 1999, 2211 and references therein.